Cellulose (2019) 26:543–555
https://doi.org/10.1007/s10570-019-02250-1

ORIGINAL PAPER

Xylanase pretreatment of wood fibers for producing cellulose nanofibrils: a comparison of different enzyme preparations

Haifeng Zhou · Franz St. John · J. Y. Zhu

Received: 29 October 2018 / Accepted: 2 January 2019 / Published online: 10 January 2019

Abstract Three commercial xylanases and an endoglucanase preparation were compared in the enzymatic pretreatment of bleached eucalyptus pulp for producing cellulose nanofibrils (CNFs) through subsequent microfluidization. Commercially provided xylanases X10A and X10B hydrolyzed more xylan than the X11 xylanase. Moreover, the average degrees of polymerization (DP) of the fibers after treatments using xylanases X10A and X10B (DP ∼ 1000) were lower than for the fibers following treatment using xylanase X11 (DP ∼ 1100). Based on protein molecular weight, the commercial xylanases X10A and X10B are both thought to be endoxylanases of glycoside hydrolase (GH) family 10 and X11, an endoxylanase of GH11. Xylanase treatment facilitated initial stage fibrillation to separate fibrils due to removal of easily accessible xylan located mainly between cellulose fibrils of micrometer size, but had no substantial effect on nanoscale fibrillation due to difficulties in removal of xylan located between nanoscale fibrils. Although electron microscopy did not show much variation among the CNF samples from different xylanase treatments, a large DP reduction associated with aggressive enzymatic treatment facilitated mechanical fibrillation and also reduced the specific tensile strength of the resulting CNF films.

Graphical abstract

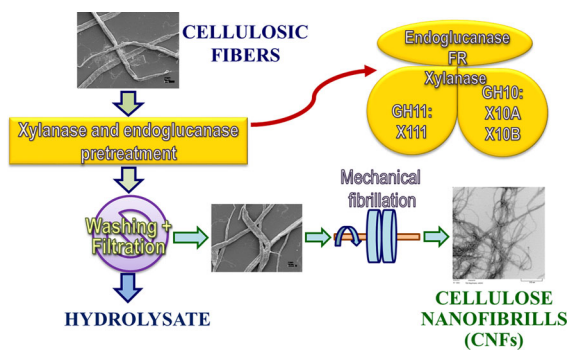

Keywords Xylanase pretreatment · Microfluidization · Cellulose nanofibrils (CNFs) · CNF films · Mechanical properties

Introduction

Cellulose is the most abundant natural polymer on earth and is highly desirable due to its high tensile strength and low density (Zhu et al. 2016). Recently,

H. Zhou
Key Laboratory of Low Carbon Energy and Chemical Engineering, College of Chemical and Environmental Engineering, Shandong University of Science and Technology, Qingdao 277590, China

H. Zhou · F. St. John · J. Y. Zhu (✉)
Forest Products Laboratory, USDA Forest Service, Madison, WI 53726, USA
e-mail: jzhu@fs.fed.us

cellulose nanomaterials including cellulose nanocrystals (CNCs) and cellulose nanofibrils (CNFs) have attracted increasing interest because of their large surface area, excellent thermomechanical properties and potential for producing a variety of value-added products (Giese et al. 2015; Mulyadi et al. 2017; Xu et al. 2013; Zheng et al. 2015). CNFs with a large aspect ratio are especially attractive for polymer reinforcement in composites. The most common approach for producing CNFs is through mechanical fibrillation of commercial pulp fibers using a homogenizer, microfluidizer, or grinder, at the expense of high energy input (Hoeger et al. 2013; Iwamoto et al. 2007; Wang et al. 2012). Chemical treatments such as catalyzed oxidation and acid hydrolysis (Naderi et al. 2014; Qin et al. 2016; Saito et al. 2006) have been applied prior to mechanical fibrillation to reduce energy consumption. However, recovery of the chemicals is a concern for economical and sustainable production of CNFs using chemical methods, especially when using expensive chemicals such as TEMPO or when using chemicals having potential environmental impact.

Enzymatic pretreatments (Hassan et al. 2018; Pääkko et al. 2007; Zhu et al. 2011), on the other hand, can be carried out using environmentally friendly conditions, and therefore are more attractive. Enzyme formulations have highly specific reactions and therefore target specific lignocellulosic linkages (Arvidsson et al. 2015; Henriksson et al. 2007; Wang et al. 2015a; Yarbrough et al. 2017). Cellulases and xylanases are the most common enzymes. Pretreatments using cellulases, such as exoglucanase and endoglucanase, for producing CNFs have been studied (Hayashi et al. 2005; Pääkkö et al. 2007; Zhu et al. 2011). Endoglucanase pretreatment will randomly cleave the cellulose β-1, 4 linkages at disordered regions of the cellulose and improve downstream fibrillation and mechanical properties of the prepared CNF films (Wang et al. 2015a, b; Yarbrough et al. 2017). Despite the limited knowledge available for lignocellulose cell wall structure, our recent study concluded that depolymerization is a necessary condition for liberating cellulose fibrils to produce CNFs (Qin et al. 2016). This supports the application of endoglucanase treatment for CNF production from pulp fibers. Furthermore, xylan is considered the main polymer that interconnects cellulose fibrils (Busse-Wicher et al. 2014), therefore xylanase treatment should facilitate fibrillation. Recently, some studies have shown that enzymes, such as xylanase and lytic polysaccharide monooxygenases (LPMO) can improve the accessibility of cellulose to enzymes (Hassan et al. 2014; Hu et al. 2018; Long et al. 2017; Saelee et al. 2016). It was found that the combination of endoglucanase, LMPO and xylanase could facilitate nanofibrillation, potentially reducing the requirement of mechanical refining (Hu et al. 2018). Moreover, the synergistic cooperation between cellulase and xylanase could change the gross fiber morphology (Hu et al. 2011, 2013). However, the potential of xylanase alone to facilitate CNF production with the desired CNF properties has not been fully investigated. Xylanase pretreatment of date palm rachis facilitated the fibrillation process and resulted in CNF films with higher strength than those from untreated fibers (Hassan et al. 2014). Xylanase treatment of sulfite pulp revealed that xylanase treatment accelerated fibrillation but did not save fibrillation energy (Hassan et al. 2018). In another study Tian et al. (Tian et al. 2017) used a mixture of xylanase and mannanase to evaluate the effects of diverse hemicellulases for enhancing refining efficiency in terms of the morphologies and physical characteristics of the resulting fibers. It was found that hemicellulase resulted in a gradual uncoiling of the fibrils from the fiber surface at multiple sites along the fiber axis. Nevertheless, the study was not focused on CNF production.

The present study investigates the effects of xylanase pretreatment of bleached kraft fibers on producing CNFs. A commercial endoglucanase is used as a control. The pretreated fibers are subjected to microfludization to produce fibrils that are characterized by degree of polymerization (DP), electron microscopy, and optical transmittance of the fibril suspension. The optical and mechanical properties of films prepared from the resulting CNFs are also compared for better understanding the CNF network from different xylanase treatments.

Materials and methods

Materials

Bleached kraft eucalyptus dry lap pulp (BEP) from Fibria (Aracruz, Brazil) was used as the feedstock for CNF production. BEP was first soaked in distilled

water for 24 h, and then disintegrated at 10% solid consistency by a lab disintegrator (TMI, Ronkonkoma, NY) at room temperature for 10,000 revolutions at 312 rpm. The disintegrated pulp was collected after vacuum filtration and stored in a freezer until use. Commercial xylanase preparations X11 (NS51024), X10A (NS51066), X10B (NS50030) and the endoglucanase FR (Fibercare) were supplied by Novozymes, Inc. (Franklinton, NC). The protein concentration of these xylanase preparations was estimated using the Bradford Assay with bovine serum albumin (Fraction V) as the standard prior to molecular weight analysis by sodium dodecyl sulfate polyacrylamide gel electrophoresis (Laemmli 1970). Xylanase activity was quantified by measurement of the increase in reducing terminus over time by the Nelson's Test (Nelson 1944) using xylose as the standard as performed previously (McCleary and McGeough 2015; St John et al. 2006). Reactions were performed using soluble beechwood xylan at 10 mg/mL, 100 mM sodium acetate pH 5.0 at 50 °C for 10 min.

The hydrolytic activities of the enzymes towards carboxymethyl cellulose (CMC) were determined from the amounts of reducing sugars released (Ghose 1987) from carboxymethyl cellulose (CMC, sodium salt, low viscosity; Sigma-Aldrich, St. Louis, MO) at 50 °C in 50 mM acetate buffer of pH 5.0 using glucose as standard. One unit (IU) of activity is defined as 1 μmol of glucose equivalent released per min. For all activity measurements, one Unit of activity (IU) is defined as the amount of enzyme capable of releasing 1 μmole of xylose or glucose equivalent per minute.

Enzymatic pretreatment of fibers

The BEP fibers were enzymatically treated by xylanases (X11, X10A, X10B) or a endoglucanase (FR) before mechanical fibrillation. The enzymatic loadings were 0.05, 0.1, 0.2, 0.3 mL/g glucan in BEP (abbreviated as mL/g in the following discussion). BEP fibers were mixed with enzymes in 50 mM acetate buffer at pH 5.0 with a solids loading of 10% (w/v), and incubated at 50 °C in a shaker (MaxQTM 4450, Thermo Scientific, Waltham, MA) at 200 rpm for 48 h. At the end of enzymatic hydrolysis, the fiber suspension was boiled for 5 min to denature the enzymes. The solids resulting from enzymatic pretreatments were washed with acetate buffer once and then with water for several times with the aid of centrifugation. The washed solids were used for analysis and mechanical fibrillation.

Analytical methods

The chemical compositions of the untreated and pretreated BEP fibers were analyzed as described previously (Luo et al. 2010). Briefly, the standard two-step acid hydrolysis procedure was used to hydrolyze polysaccharides. The acid hydrolysates were analyzed by ion chromatography with pulsed amperometric detection (ICS-5000, Dionex, Sunnyvale, CA). Separately, enzymatic hydrolysates of BEP fibers were analyzed for xylose, xylobiose, and xylotriose using an HPLC system (Ultimate 3000, Thermo Scientific, Sunnyvale, CA), equipped with a BioRad Aminex HPX-87P column (300 mm × 7.8 mm) operated at 80 °C and an RI (RI101, Shodex) detector as described previously (Zhou et al. 2013).

Mechanical fibrillation by microfluidization

BEP pulp fibers with or without enzymatic pretreatment were fibrillated using a microfluidizer (M-110EH, Microfluidics Corp., Westwood, MA). The fiber slurry of 0.3% (w/v) was passed through two different sized chambers, first through a 200 μm chamber for 40 times at 250 bar, and then up to an additional 20 times through a 87 μm chamber at 1500 bar.

CNF suspension light transmittance and CNF film optical properties

Light transmittance values of the mechanically fibrillated CNF suspensions (0.1%, w/v) were measured at 600 nm using a spectrophotometer (Model 8453, Agilent Technologies, Inc., USA). Brightness and opacity of the CNF films were measured by TAPPI Standard Test Method T519 om-06.

Determination of degree of polymerization

The DPs of the enzymatically treated fiber samples were measured according to TAPPI Standard Test Method T230 om-99 (TAPPI 1999). Vacuum dried cellulosic solids of 0.1 g were first dispersed in 10 mL distilled water, and then added 10 mL of 1 M cupriethylenediamine solution. The viscosity of the

resulting solution was determined using a capillary viscometer. The DP of the cellulose was calculated using the following expression (Mazumder et al. 2000): $DP^{0.905} = 0.75$ (954 logX-325), where X is the measured viscosity.

Scanning and transmission electron microscopy and imaging

Fibril specimens were prepared by drying drops of an aqueous slurry of 0.1 g/L on aluminum mounts for scanning electron microscopy (SEM). All specimens were sputter-coated with gold to provide adequate conductivity for examination in a Zeiss EVO 40 SEM (Carl Zeiss NTS, Peabody, MA) under ultrahigh vacuum conditions. For transmission electron microscopy (TEM) analyses, aqueous CNF suspensions (0.3 g/L) were further diluted and sonicated to disperse the fibrils. TEM grids (ultrathin carbon films supported by fenestrated carbon films) were floated on drops of approximately 5 µL sample for 1–2 min. They were then swished through two consecutive 250 µL drops of 2% aqueous uranyl acetate. Excess stain removal by capillary action and gentle blotting resulted in negatively stained particles. The samples were imaged using a Philips CM100 transmission electron microscope (FEI Company, Portland OR) with an accelerating potential of 100 keV. Images were captured on Kodak SO-163 electron image film and later scanned digitally at 600 dpi resolution.

Preparation of CNF films

CNF films were prepared according to the procedure described previously (Wang et al. 2015b) by pressure filtration of 2 g (oven dry) of CNFs in suspension at a consistency of 0.3 wt%. Prior to filtration, the suspension was kept stirring for 12 h to ensure good dispersion. All films were filtered at room temperature under air pressure of 3.45 bar in a Hazardous Waste Filtration system of 142 mm inner diameter (YT30142HW, Millipore Corporation, USA). The filtration membrane (JVWP14225, Millipore Corporation, USA) had a reported pore size of 0.1 µm supported by filter paper (P2, Fisher Scientific, USA). After filtration, the wet film was stacked between wax-coated papers that were changed periodically. The assembly was then sandwiched between two steel plates, and a 23 kg weight was placed on the plates at room temperature for 24 h to minimize deformation (Qing et al. 2013). When the solids content of the film reached approximately 80–90%, the film was then dried in an oven at 60 °C for 24 h pressed by 23 kg weight.

Mechanical testing of CNF films

The tensile properties of the CNF films were tested according to ASTM D638–10. The specimens were cut to conform to ASTM D638–10 type V dog bone shape using a special die (Qualitest, FL, USA) and were subsequently conditioned at 50% RH and 23 °C for at least one week prior to testing in a humidity controlled room at 50% RH and 23 °C. The tests were performed on an Instron Model 5566 equipped with a 440 N load cell at a crosshead speed of 10 mm/min. Each film sample had twelve specimens prepared for the test. An LX 500 laser extensometer (MTS Systems Corporation, MN, USA) was used to determine the displacement with sampling frequency at 10 Hz. The laser recorded the displacement between two strips of reflective tape initially placed approximately 8 mm apart on the necked-down region of the dog-bone specimens. Strain was calculated from the determined displacement and initial gage length. The data were fit to a hyperbolic tangent in order to extract the tensile modulus as the initial slope of the stress–strain curve. Reported results were averages of those valid measurements from at least six specimens per sample.

Results and discussion

Characterization of xylanases and endoglucanase FR

SDS-Page analyses of the enzymes are shown in Fig. 1. Based on their apparent molecular weight, X10A and X10B are both likely to be GH10 endoxylanases that also have a carbohydrate binding module (CBM) attached. In a similar manner, based on the apparent molecular weight X11 is most likely a GH11 endoxylanase also appended with a CBM. These three endoxylanases have different xylanase activities as listed in Table 1 but neither has cellulase activity. X11 has a highest xylanase activity of 3160 U/mL among all three xylanases, while the xylanase activity of X10B was the lowest of 2013 U/mL. The FR CMC

activity of 21 IU/mg at 50 °C and FR SDS-PAGE were from our previous study (Wang et al. 2015a).

Xylanases and endoglucanase pretreatments of BEP fibers

Endoxylanases hydrolyze xylan to form xylooligosaccharides (Zhang et al. 2013). Xylose and the xylooligosaccharide concentrations in the BEP fiber xylanase hydrolysates at varied xylanase loadings are shown in Fig. 2. The resultant hydrolysis product distributions were very different among various treatments using the three xylanases, especially for the xylanases from different apparent families. The two xylanases, X10A and X10B, which, from molecular weight determination are predicted to both be GH10 endoxylanases (Table 1) showed only minor variations in their hydrolysis products. Compared to X10A, X10B performed poorly at low xylanase loadings of < 0.2 mL/g but better at loading of 0.3 mL/g, while treatment using X11 which we predict to derive from endoxylanase family GH11, resulted in substantially different hydrolysis products compared to treatments using the GH10 xylanases. The putative GH11 xylanase produced a lower amount of total soluble sugars (including xylose, xylobiose and xylotriose) than the two GH10 xylanases did. Furthermore, the GH11 xylanase was not effective in hydrolyzing xylotriose and resulted in substantially more xylotriose in the hydrolysates. The two putative GH10 xylanases effectively hydrolyzed xylotriose to a negligible level. Results in Fig. 2 also indicate that xylobiose was the main product for all three xylanase pretreatments at all enzyme loading levels. The xylobiose concentrations were 1.4, 2.0 and 2.2 g/L with X11, X10A and X10B pretreatment at 0.3 mL/g xylanase loading, respectively. The observed oligosaccharide differences are consistent with what is known regarding the differences between these two distinct types of endoxylanases (Liao et al. 2015). Increasing xylanase loading increased overall sugar release for the putative GH11 xylanase X11 and GH10 xylanase X10B, but had an indiscernible effect using the putative GH10 X10A. At a xylanase loading of 0.3 mL/g, sugar release from the three xylanase treatments followed the order of X11 $<$ X10A $<$ X10B. This xylanase loading was chosen for CNF production.

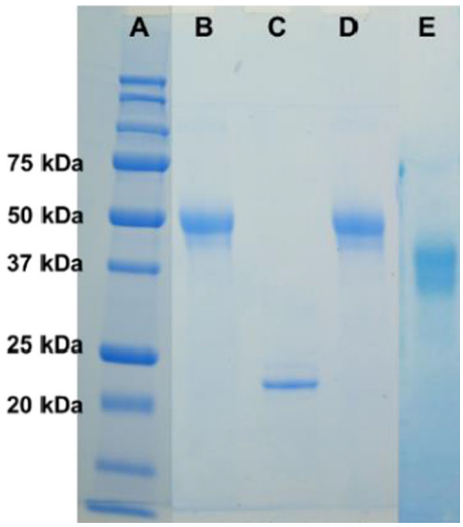

Fig. 1 SDS-PAGE of the three xylanases and FR. **A**: Standard; **B**: X10B; **C**: X11; **D**: X10A; **E**: FR

The chemical compositions of the BEP fibers treated by three xylanases at 0.3 mL/g were analyzed and the solid yields from treatments were determined. Approximately 4% of the fibers were lost as a result of xylanase pretreatments. Endoglucanase treatment using FR did not remove xylan but solubilized approximately 2.5% of the glucan as expected, which resulted in minimal fiber loss. The near 100% fiber yield under FR treatment reported in Table 2 may be due to errors in gravimetric measurement. As listed in Table 2, xylanase treatment only reduced xylan content of BEP fibers without solubilizing glucan. The measured total xylan dissolutions were the same at approximately 22% for all three xylanase treatments. Xylan dissolution was 18% based on the sum of the concentrations of xylose, xylobiose, and xylotriose at 2.6 g/L shown in Fig. 2, below but consistent with the 22% determined from the yields and compositions of the hydrolyzed BEP fibers. The difference is mainly attributed to the high order (> 3) xylooligomers that were not measured. The amount of xylan dissolution was greater than that reported by Tian et al. (2017).

The DPs of the enzymatically treated BEP fibers as listed in Table 2 also reflect the difference in the actions of the enzymes used. GH11 endoxylanases (e.g. X11) as also observed from the data presented in Fig. 2 are known to be less effective in xylan hydrolysis around xylan main-chain substitutions compared to GH10 endoxylanases, an observation which may also extend to steric accessibility from

Table 1 Characteristics of xylanases and endoglucanase FR

Enzyme	Xylanase family[a]	Xylanase activity (U/mL)	CMC activity (IU/mg)	Protein content (mg/mL)
NS51024 (X11)	GH11	3160	ND[c]	0.71 ± 0.02
NS51066 (X10A)	GH10	2846	ND	7.36 ± 0.17
NS50030 (X10B)	GH10	2013	ND	8.02 ± 0.02
Fibercare (FR)	NA[b]	NA	21.04	6.20 ± 0.35

[a]Glycoside hydrolase family predicted based on the determined molecular weight

[b]Not applicable

[c]Not determined

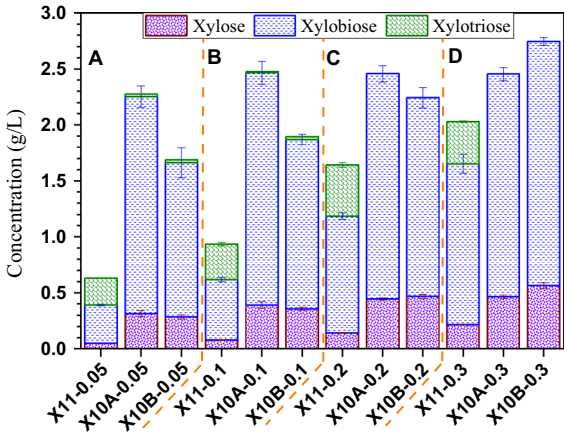

Fig. 2 Xylose and xylooligomer concentrations in enzymatic hydrolysates from different xylanase treatments of BEP fibers for 48 h at different dosages. Xylanase loadings (mL/g glucan): **A** = 0.05; **B** = 0.1; **C** = 0.2; **D** = 0.3

cellulose association (Biely et al. 1997). The two GH10 family xylanase X10A and X10B were more aggressive and reduced DP by approximately 16–18%, or from 1235 to slightly over 1000. The slight variation in DP reduction between the treatments using the two GH10 xylanases was not statistically significant based on a *t* test, though it was consistent with the variations in the sums of xylose and xylobiose measured in the treatment hydrolysates shown in Fig. 2. Endoglucanase FR, known to aggressively cut cellulose chains, reduced DP from 1235 to 689 or by approximately 44%. DP reduction should facilitate nanofibrillation as previously suggested (Qin et al. 2016).

In order to obtain a better understanding of the effect of enzymatic pretreatment on CNF production, SEM was used to reveal the morphologies of BEP fibers as shown in Fig. 3 (left and middle panels A–E, a–e). Compared with the untreated fibers, careful visual observation show minor effects on surface morphology such as surface roughness and small cracks. This is in agreement with literature studies indicating grooves, cracks or porosities in the less crystalline regions with xylanase treatment (Roncero et al. 2005). However, no substantial variations in fiber morphology were observed among differently treated fibers.

CNF properties

Suspensions of fibers or CNFs at 0.1 w/v% in glass vials of 10 mm in diameter are shown in Fig. 3 (right panel A′–E′). A black background was applied to visually exhibit the dispersity of the CNF suspensions. All fibers without microfluidization settled to the bottom of the vials. Fibrillation through microfluidization enhanced fibril dispersity. It is interesting to note that at low degree of fibrillation (through the 200 μm chamber only at 40 and especially 20 passes), the three xylanase-treated fibril suspensions (Fig. 3B′–D′) were slightly more transparent and had less precipitation than the fibril suspensions without treatment (Fig. 3A′) or with endoglucanase treatment (Fig. 3E′ 20 passes) that did not remove xylan. This indicates xylanase treatment facilitated initial fibrillation which mainly separates fibrils of micrometer scale. According to the microfibril ultrastructural model (Fengel 1970), we postulate that most xylan removal by xylanase treatments occurred among fibrils of microscale, i.e., these xylans are more accessible than the remaining xylans that are located between fibrils of nanometer scale. As a result, xylanase treatment is effective in the initial stage of

Table 2 Chemical compositions and solid yields of enzymatic pretreated BEP fibers at xylanase and endoglucanase (FR) loadings of 0.3 mL/g

Sample	Solids yield (%)	DP	K Lignin (%)	Galactan (%)	Glucan (%)	Xylan (%)	Mannan (%)
BEP	100	1235 ± 43	0.9 ± 0.30	0.1 ± 0.01	74.5 ± 1.53	13.6 ± 0.41	0.1 ± 0.03
X11	95.78 ± 0.14	1126 ± 12	1.1 ± 0.62	0.1 ± 0.09	79.3 ± 0.26	11.0 ± 0.02	0.1 ± 0.15
X10A	95.62 ± 0.17	1034 ± 16	0.4 ± 0.05	ND	78.9 ± 0.16	10.7 ± 0.02	ND
X10B	96.01 ± 0.13	1011 ± 11	0.8 ± 0.02	ND	79.1 ± 1.47	10.8 ± 0.38	ND
FR	99.45 ± 0.18	689 ± 11	2.6 ± 1.49	0.1 ± 0.05	72.8 ± 1.71	13.7 ± 0.21	0.1 ± 0.10

fibrillation, but may not be effective for nanoscale fibrillation.

To further reduce the fibril size to the nanoscale level through extensive fibrillation, endoglucanase treatment (FR Fig. 3E′) is more effective than xylanase. After 40 passes, all fibrils were well dispersed in water. The fibrils with endoglucanase FR pretreatment had much better dispersity and transparency than the other samples (compare Fig. 3E′ with A′–D′). The fibril suspensions without treatment were most opaque (or had large fibril size). These images suggest that DP reduction by enzymatic treatment facilitated nanofibrillation, in agreement with our early study (Qin et al. 2016).

The above discussion suggests that application of xylanase treatment supplemented by endoglcanase treatment should facilitate nanofibrillation, in agreement with a recent study (Hu et al. 2018).

Light transmittances (at 600 nm) of well dispersed fibril suspensions can be used as another measure of the degree of fibrillation. Optical transmittance for CNFs with an additional 10 passes through the 87 μm, i.e., 40 + 20 passes, improved over those from 40 + 10 passes as shown in Fig. 4, though visual observation in Fig. 3 (left panel A′–E′) cannot discern the differences. Endoglucanase FR treatment resulted in CNF suspensions with the highest optical transmittance, in agreement with visual observation in Fig. 3. GH10 xylanase X10A and X10B treatments that produced more xylan dissolution (Table 2) than GH11 xylanase X11 resulted in CNF suspensions with higher optical transmittance than the CNF from X11 treatment. Large reductions in DP by aggressive enzymatic treatment, especially by endoglucanase (FR) treatment, resulted in increased optical transmittance of the fibril suspensions (Fig. 4). In general, the reduction in fiber DP by aggressive enzymatic treatment resulted in CNFs with a low DP (Table 2; Fig. 4). Endoglucanase FR that is known to cut cellulose chains resulting in the lowest fiber DP as well as the lowest CNF DP of only approximately 300, and the most transparent fibril suspension.

Scanning electron microscopy (SEM) images of BEP fibrils from microfluidization of various passes of the untreated and enzymatically pretreated BEP fibers are shown in Fig. 5. After 40 passes through the 200 μm chamber, the diameters of the fibrils were still greater than 1 μm, some of which were almost 10 μm (Fig. 5 left panel). Microfluidization decreased the average length of the fibrils. The lengths of fibrils from untreated BEP fibers after 40 passes of microfluidization were approximately 650–1300 μm (Fig. 5A40). The average lengths of fibrils were approximately 600–1100, 400–900, and 300–900 μm with X11, X10A and X10B pretreatment, respectively (Fig. 5A40–E40), consistent with their corresponding DPs of the treated fibers (Table 2) as well as the DPs of their corresponding fibrils from 40 + 20 passes microfluidization discussed above (Fig. 4). Very long fibrils of > 1000 μm can be clearly seen from xylanase pretreated samples. The lengths of fibrils from endoglucanase FR pretreated fibers were much more uniform between 5 and 40 μm (Fig. 5E40), much shorter than those from the untreated and xylanases pretreated fibers, consistent with fibril DP shown in Fig. 4.

After additional processing of 10 passes through the 87 μm chamber (40 + 10), the fibril diameters decreased substantially as shown in the middle panel of Fig. 5. The fibril lengths were much longer and could not be determined by SEM. However, no clear difference could be observed between the untreated and different xylanase treated fibrils from SEM measurements. The fibrils from endoglucanase FR

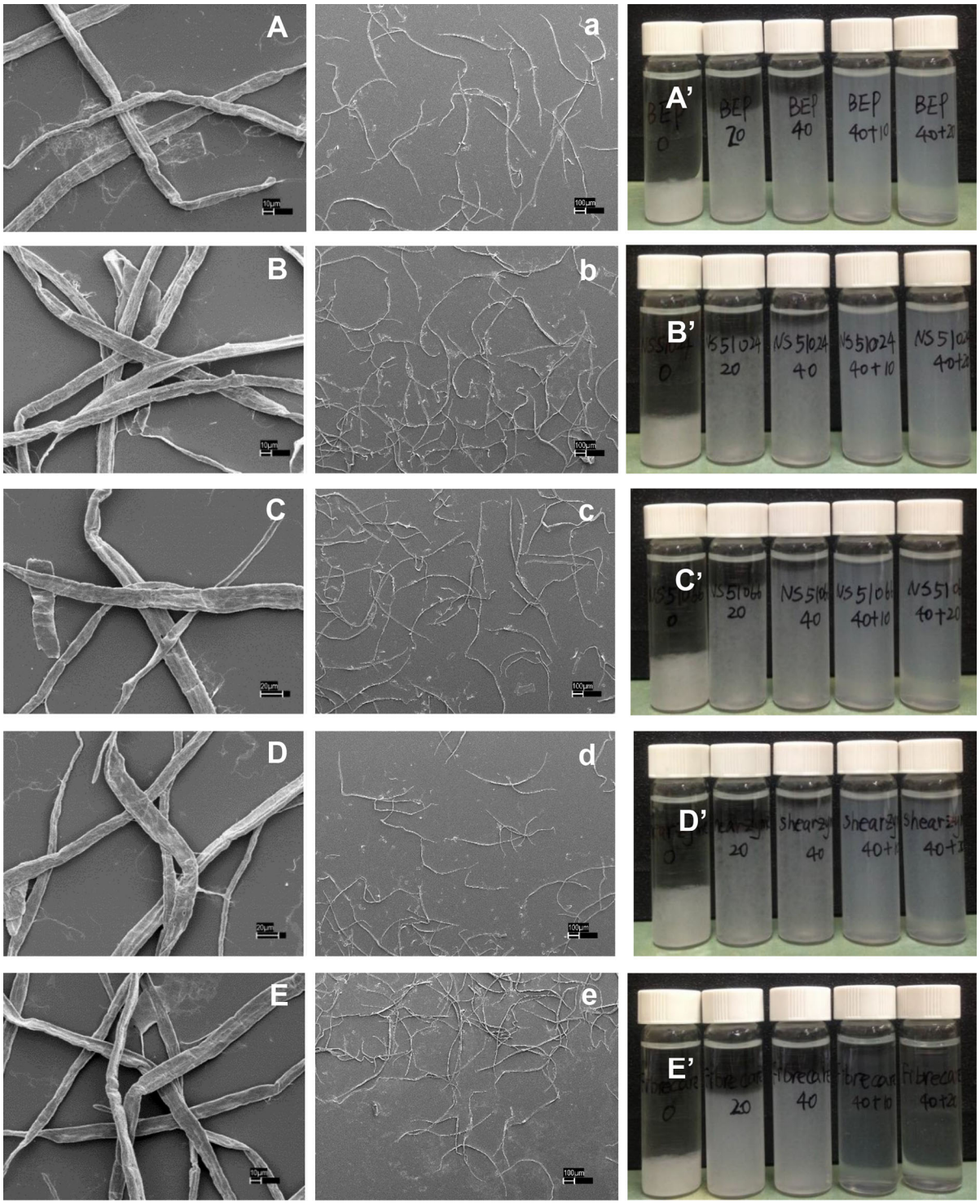

Fig. 3 SEM images of enzymatically treated fibers (left panel) and images of suspensions of fibers or CNFs from enzymatically treated fibers with subsequent microfluidization (right panel, passes through 200 μm + 87 μm chambers for bottles from left to right: 0 + 0, 20 + 0, 40 + 0, 40 + 10, 40 + 20, respectively). **A**, **a**, **A′**: untreated; **B**, **b**, **B′**: X11; **C**, **c**, **C′**: X10A; **D**, **d**, **D′**: X10B; **E**, **e**, **E′**: FR

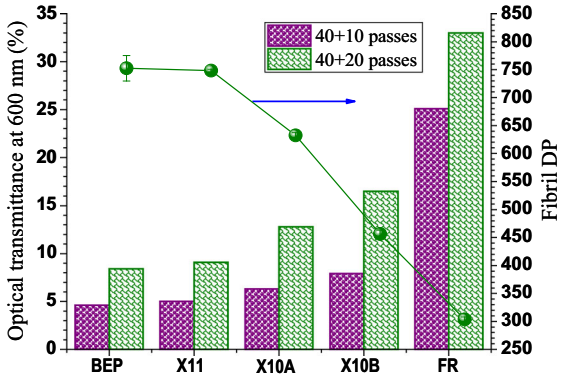

Fig. 4 Comparisons of CNF DP and optical transmittances of CNF suspensions at 0.1 w/v % among CNFs from microfluidization of different enzymatically treatments BEP fibers at two fibrillation degrees: 10 and 20 passes through the 87 µm chamber after 40 passes through the 200 µm chamber

treated fibers were around 10 µm (Fig. 3E40 + 10). With 20 passes through the 87 µm chamber (40 + 20 passes), the physical dimensions of the fibrils were further decreased as shown in the right panel of Fig. 5. The effect of extended microfluidization was clearly demonstrated. Some large micrometer-scale fibers nevertheless existed in all samples.

TEM images of CNFs from 40 + 20 passes through microfluidization were obtained to provide more detailed morphological information. As expected, the CNFs from untreated and xylanases pretreated BEP fibers were very long, therefore CNF lengths were not quantified and only diameters were analyzed from TEM. With extensive mechanical fibrillation, large variations in CNF diameters were not observed among the three xylanase treatments. This is because xylanase treatment mainly affected the initial stage of fibrillation for microscale fibrils as discussed previously due to the removal of easily accessible xylan embedded between microscale fibrils. Extensive fibrillation using 40 + 20 passes fibrillated the fibers into nanoscale sized fibrils.

The diameters of CNFs from untreated BEP fibers were in a range of 2–20 nm (Fig. 6A′–D′). It is worth mentioning that thick and wide fibril bundles of 45–65 nm were present in all samples (Fig. 5 right panel). This was in agreement with previous work (Hassan et al. 2014) that found the widths of the fibrils from xylanase treated fibers were 60–85 nm. It should be noted that these fibril bundles were not reflected in Fig. 6A′–D′ as fibrils were manually picked (biased) for the distribution calculations. The application of endoglucase FR cut the cellulose chains, resulting in shorter fibrils than the untreated and xylanase treated samples (Fig. 6E), in agreement with DP data presented in Fig. 4. Moreover, fibril diameters from FR pretreated fibers were thinner and more uniform, from 5 to 11 nm (Fig. 6E and E′) than fibrils from untreated and xylanase treated fibers, because cellulose depolymerization facilitated nanoscale fibrillation as discussed earlier (Qin et al. 2016).

Properties of CNF films

CNF films were made of fibrils from extensive fibrillation (40 + 20 passes). As discussed previously, xylanase treatments did not show observable effects in CNF morphology through extensive fibrillation. Brightness and opacities along with grammages (basis weights) of CNF films were measured as listed in Table 3. No significant changes were observed in the brightness and opacity of the CNF films with xylanase pretreatments. The opacity data of CNF films were in good agreement with the light transmittance data of the CNFs (Fig. 4). The opacity of CNF films from FR pretreatment could be as low as 12.4% due to shortened fibrils, compared with 25.2% from untreated BEP.

The physical properties of the films were also listed in Table 3. Enzymatic treatment reduced specific tensile strength. The reduction seemed proportional to the extent of treatment or DP reduction, i.e., aggressive treatment using FR that substantially deploymerized cellulose (Fig. 4) had a major reduction in tensile strength. GH11 family xylanase treatment led to a minimal reduction in cellulose DP (Fig. 4), resulting in maximal specific tensile strength among all treated samples. Specific tensile modulus was increased with aggressive FR treatment. However, different xylanase treatments had no noticeable effects on specific tensile modulus. According to discussions presented previously, xylanase treatment is effective for initial stage of fibrillation or fibrillation at the microscale, but did not have substantial effects on morphology of nanofibrils from extensive fibrillation at nanoscale. As a result, films made from different xylanase treatments had similar optical and mechanical properties.

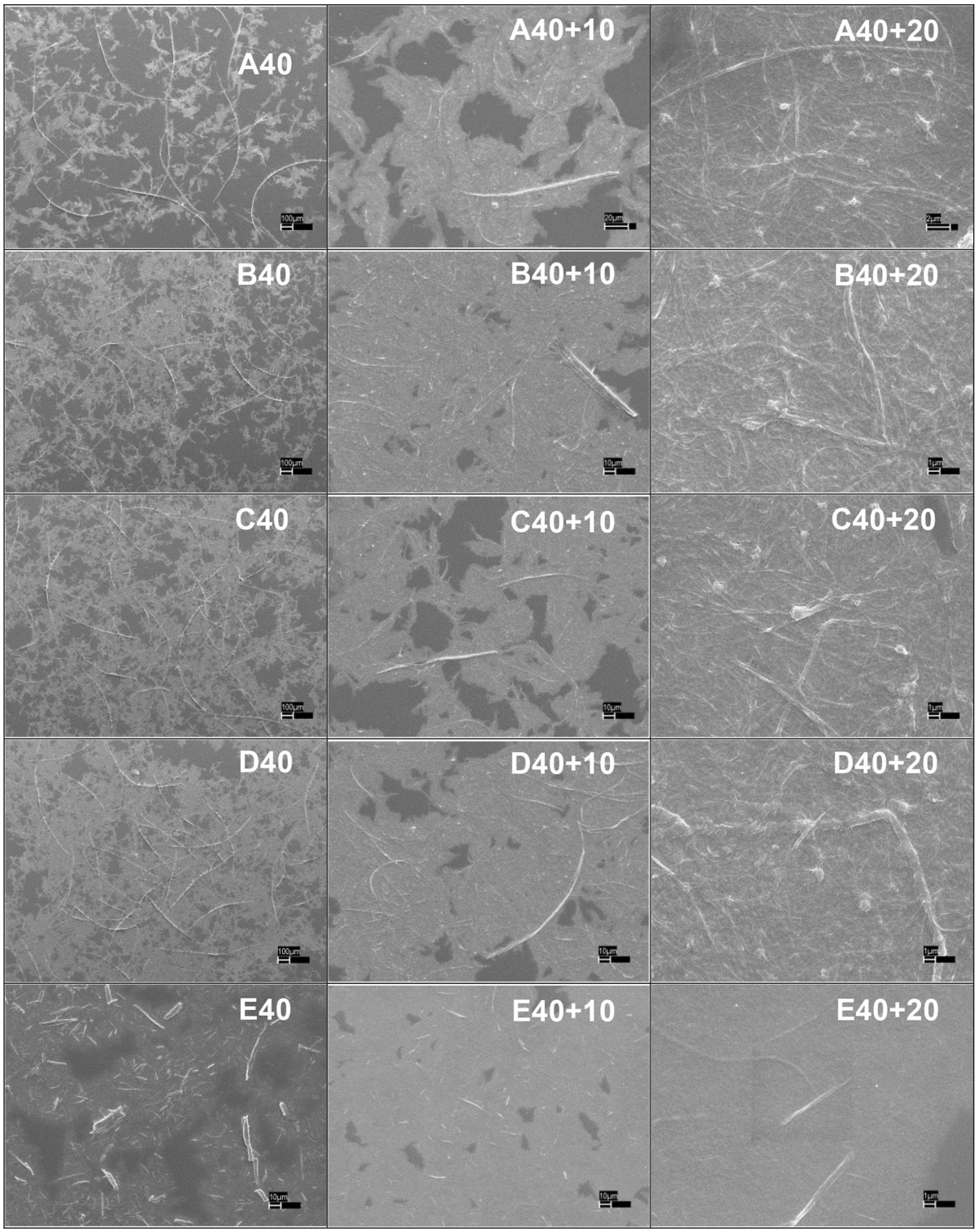
A40
A40+10
A40+20
B40
B40+10
B40+20
C40
C40+10
C40+20
D40
D40+10
D40+20
E40
E40+10
E40+20

◀**Fig. 5** SEM images of BEP fibrils from different passes of microfluidization using BEP fibers with and without enzymatic treatments. Left Panel: 40 + 0 passes (scale bars =100 μm, except for E40: = 10 μm); middle panel: 40 + 10 passes (all scale bars = 10 μm, except for A40 + 10: = 20 μm); right panel: 40 + 20 passes (all scale bars = 1 μm, except for A40 + 20: = 2 μm), through the 200 μm and 87 μm chamber, respectively. A: untreated BEP fibers; B: X11; C: X10A; D: X10B; E: FR

Conclusions

Xylanase treatment of fibers resulted in minimal depolymerization of cellulose and produced CNFs from subsequent mechanical fibrillation with longer length than those from endoglucanase treated fibers. The GH10 family xylanase showed more aggressive treatment than the GH11 family xylanase and resulted in slightly more deploymerization of cellulose. Cellulose DP reduction facilitated mechanical fibrillation as can be seen from the optical transmittance of the CNF suspensions. A CNF suspension from treated fibers with lower DP had a higher optical transmittance. CNF films made from CNFs with lower DP had a low specific tensile strength. This suggests xylanase treatment is preferred to endoglucanase for producing CNFs as a polymer reinforcement. Xylanase treatment can facilitate the initial stage of fibrillation for producing micro scale fibrils, but not for producing nanometer scale fibrils due to the fact that the easily accessible xylan removed by xylanase is embedded between fibrils of microscale. To facilitate nanoscale fibrillation, cellulose depolymerization by endoglucanase is more effective. A combination of first xylanase treatment with subsequent endoglucanase treatment may be devised to reduce energy in nanofibrillation.

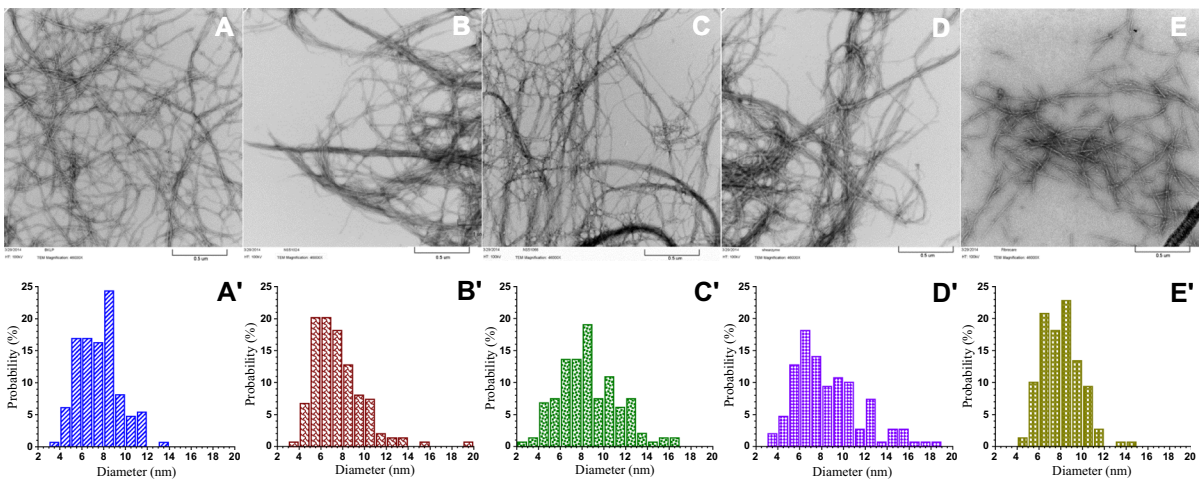

Fig. 6 TEM images (top panel) and diameter distributions (bottom panel) of CNFs from BEP fibers with and without enzymatic pretreatment after subsequent 40 + 20 passes of microfluidization. **A** and **A′**: untreated BEP fibers; **B** and **B′**: X11; **C** and **C′** X10A; **D** and **D′**: X10B; **E** and **E′**: FR. All scale bars = 0.5 μm

Table 3 Optical and physical properties of CNF films

Film	Grammage (g/m^2)	Brightness (%)	Opacity (%)	Specific tensile (MN m/kg)	Specific modulus (MN m/kg)
BEP	65.1	47.9 ± 0.0	25.2 ± 0.1	158.9 ± 15.9	3.21 ± 0.35
X11	59.4	48.5 ± 0.1	27.5 ± 0.1	141.8 ± 14.4	3.23 ± 0.37
X10A	55.5	47.1 ± 0.1	25.1 ± 0.1	140.4 ± 8.5	3.44 ± 0.29
X10B	52.5	48.1 ± 0.1	25.1 ± 0.2	120.0 ± 10.4	3.44 ± 0.42
FR	49.1	43.8 ± 0.2	12.4 ± 0.2	117.8 ± 12.1	4.29 ± 0.51

Acknowledgments This work was conducted at the USDA Forest Products Lab (FPL) while HZ was a visiting student under the sponsorship of Chinese Scholarship Council (CSC). We would like to acknowledge Dr. Ron Sable of FPL for conducting tensile tests of CNF films. HZ would also like to acknowledge the financial support of the National Natural Science Foundation of China (21506117), the Key Research and Development Plan of Shandong (2018GGX104015), the Applied Basic Research Programs of Qingdao (17–1-1–23-jch) and SDUST Research Fund (2018YQJH102 and 2015RCJJ008).

References

Arvidsson R, Nguyen D, Svanström M (2015) Life cycle assessment of cellulose nanofibrils production by mechanical treatment and two different pretreatment processes. Environ Sci Technol 49:6881–6890

Biely P, Vršanská M, Tenkanen M, Kluepfel D (1997) Endo-beta-1,4-xylanase families: differences in catalytic properties. J Biotechnol 57:151–166

Busse-Wicher M et al (2014) The pattern of xylan acetylation suggests xylan may interact with cellulose microfibrils as a twofold helical screw in the secondary plant cell wall of *Arabidopsis thaliana*. Plant Journal 79:492–506

Fengel D (1970) Ultrastructural behavior of cell wall polysaccharides. Tappi 53:497–503

Ghose TK (1987) Measurement of cellulase activities. Pure Appl Chem 59:257–268

Giese M, Blusch LK, Khan MK, MacLachlan MJ (2015) Functional materials from cellulose-derived liquid–crystal templates. Angew Chem Int Edit 54:2888–2910

Hassan ML, Bras J, Hassan EA, Silard C, Mauret E (2014) Enzyme-assisted isolation of microfibrillated cellulose from date palm fruit stalks. Ind Crop Prod 55:102–108

Hassan M, Berglund L, Hassan E, Abou-Zeid R, Oksman K (2018) Effect of xylanase pretreatment of rice straw unbleached soda and neutral sulfite pulps on isolation of nanofibers and their properties. Cellulose 25:2939–2953

Hayashi N, Kondo T, Ishihara M (2005) Enzymatically produced nano-ordered short elements containing cellulose Iβ crystalline domains. Carbohydr Polym 61:191–197

Henriksson M, Henriksson G, Berglund LA, Lindström T (2007) An environmentally friendly method for enzyme-assisted preparation of microfibrillated cellulose (MFC) nanofibers. Eur Polym J 43:3434–3441

Hoeger IC, Nair SS, Ragauskas AJ, Deng Y, Rojas OJ, Zhu JY (2013) Mechanical deconstruction of lignocellulose cell walls and their enzymatic saccharification. Cellulose 20:807–818

Hu J, Arantes V, Saddler JN (2011) The enhancement of enzymatic hydrolysis of lignocellulosic substrates by the addition of accessory enzymes such as xylanase: Is it an additive or synergistic effect? Biotechnol Biofuels 4:36

Hu J, Arantes V, Pribowo A, Saddler JN (2013) The synergistic action of accessory enzymes enhances the hydrolytic potential of a "cellulase mixture" but is highly substrate specific. Biotechnol Biofuels 6:112

Hu J, Tian D, Renneckar S, Saddler JN (2018) Enzyme mediated nanofibrillation of cellulose by the synergistic actions of an endoglucanase, lytic polysaccharide monooxygenase (LPMO) and xylanase. Sci Rep 8:3195

Iwamoto S, Nakagaito AN, Yano H (2007) Nano-fibrillation of pulp fibers for the processing of transparent nanocomposites. Appl Phys A Mater Sci Process 89:461–466

Laemmli UK (1970) Cleavage of structural proteins during the assembly of the head of bacteriophage T4. Nature 227:680–685

Liao H, Zheng H, Li S, Wei Z, Mei X, Ma H, Shen Q, Xu Y (2015) Functional diversity and properties of multiple xylanases from Penicillium oxalicum GZ-2. Sci Rep 5:12631. https://doi.org/10.1038/srep12631

Long L, Tian D, Hu J, Wang F, Saddler J (2017) A xylanase-aided enzymatic pretreatment facilitates cellulose nanofibrillation. Bioresour Technol 243:898–904

Luo X, Gleisner R, Tian S, Negron J, Zhu W, Horn E, Pan X, Zhu J (2010) Evaluation of mountain beetle-infested lodgepole pine for cellulosic ethanol production by sulfite pretreatment to overcome recalcitrance of lignocellulose. Ind Eng Chem Res 49(17):8258–8266

Mazumder BB, Ohtani Y, Cheng Z, Sameshima K (2000) Combination treatment of kenaf bast fiber for high viscosity pulp. J Wood Sci 46:364–370

McCleary BV, McGeough P (2015) A comparison of polysaccharide substrates and reducing sugar methods for the measurement of endo-1, 4-β-xylanase. Appl Biochem Biotechnol 177:1152–1163

Mulyadi A, Zhang Z, Dutzer M, Liu W, Deng Y (2017) Facile approach for synthesis of doped carbon electrocatalyst from cellulose nanofibrils toward high-performance metal-free oxygen reduction and hydrogen evolution. Nano Energy 32:336–346

Naderi A, Lindström T, Sundström J (2014) Carboxymethylated nanofibrillated cellulose: rheological studies. Cellulose 21:1561–1571

Nelson N (1944) A photometric adaptation of the Somogyi method for the determination of glucose. J Biol Chem 153:375–379

Pääkko M et al (2007) Enzymatic hydrolysis combined with mechanical shearing and high-pressure homogenization for nanoscale cellulose fibrils and strong gels. Biomacromol 8:1934–1941

Qin Y, Qiu X, Zhu JY (2016) Understanding longitudinal wood fiber ultra-structure for producing cellulose nanofibrils using disk milling with dilute acid prehydrolysis. Sci Rep 6:35602

Qing Y, Sabo R, Cai Z, Wu Y (2013) Resin impregnation of cellulose nanofibril films facilitated by water swelling. Cellulose 20:303–313

Roncero MB, Torres AL, Colom JF, Vidal T (2005) The effect of xylanase on lignocellulosic components during the bleaching of wood pulps. Bioresour Technol 96:21–30

Saelee K, Yingkamhaeng N, Nimchua T, Sukyai P (2016) An environmentally friendly xylanase-assisted pretreatment for cellulose nanofibrils isolation from sugarcane bagasse by high-pressure homogenization. Ind Crop Prod 82:149–160

Saito T, Nishiyama Y, Putaux JL, Vignon M, Isogai A (2006) Homogeneous suspensions of individualized microfibrils

from TEMPO-catalyzed oxidation of native cellulose. Biomacromol 7:1687–1691

St John FJ, Rice JD, Preston JF (2006) Characterization of XynC from *Bacillus subtilis* subsp. subtilis strain 168 and analysis of its role in depolymerization of glucuronoxylan. J Bacteriol 188:8617–8626

Tian X, Lu P, Song X, Nie S, Liu Y, Liu M, Wang Z (2017) Enzyme-assisted mechanical production of microfibrillated cellulose from Northern Bleached Softwood Kraft pulp. Cellulose 24:3929–3942

Wang QQ, Zhu JY, Gleisner R, Kuster TA, Baxa U, McNeil SE (2012) Morphological development of cellulose fibrils of a bleached eucalyptus pulp by mechanical fibrillation. Cellulose 19:1631–1643

Wang W, Mozuch MD, Sabo RC, Kersten P, Zhu JY, Jin Y (2015a) Production of cellulose nanofibrils from bleached eucalyptus fibers by hyperthermostable endoglucanase treatment and subsequent microfluidization. Cellulose 22:351–361

Wang W, Sabo RC, Mozuch MD, Kersten P, Zhu JY, Jin Y (2015b) Physical and mechanical properties of cellulose nanofibril films from bleached eucalyptus pulp by endoglucanase treatment and microfluidization. J Polym Environ 23:551–558

Xu X, Liu F, Jiang L, Zhu JY, Haagenson D, Wiesenborn DP (2013) Cellulose nanocrystals versus cellulose nanofibrils: a comparative study on their microstructures and effects as polymer reinforcing agents. ACS Appl Mater Interfaces 5:2999–3009

Yarbrough JM et al (2017) Multifunctional cellulolytic enzymes outperform processive fungal cellulases for coproduction of nanocellulose and biofuels. ACS Nano 11:3101–3109

Zhang C, Zhuang X, Wang ZJ, Matt F, John FS, Zhu JY (2013) Xylanase supplementation on enzymatic saccharification of dilute acid pretreated poplars at different severities. Cellulose 20:1937–1946

Zheng Q, Cai Z, Ma Z, Gong S (2015) Cellulose nanofibril/reduced graphene oxide/carbon nanotube hybrid aerogels for highly flexible and all-solid-state supercapacitors. ACS Appl Mater Interfaces 7:3263–3271

Zhou H et al (2013) Bioconversion of beetle-killed lodgepole pine using SPORL: process scale-up design, lignin coproduct, and high solids fermentation without detoxification. Ind Eng Chem Res 52:16057–16065

Zhu JY, Sabo R, Luo X (2011) Integrated production of nanofibrillated cellulose and cellulosic biofuel (ethanol) by enzymatic fractionation of wood fibers. Green Chem 13:1339–1344

Zhu H et al (2016) Wood-derived materials for green electronics, biological devices, and energy applications. Chem Rev 116:9305–9374